*Int. J. Solids Structures*, 1968, Vol. 4, pp. 61 to 74. Pergamon Press. Printed in Great Britain

# LARGE PLASTIC DEFORMATIONS OF REINFORCED CONCRETE SLABS

M. JANAS*

Polish Academy of Sciences, Warsaw, Poland

**Abstract**—Plastic response of reinforced concrete slabs is analyzed, including membrane effects and geometry changes at large deflections. Based on the flow theory of rigid–plastic bodies, load–deflection relations are derived, starting from the initial compression ("arching action") in laterally restrained slabs, up to the overall membrane tension and cracking. The kinematical approach is applied, using energy or/and equilibrium methods, with the initial collapse mode assumed to be preserved at large deflections. Examples of clamped strip, square and circular slabs are presented, and the comparison with the approach based on the deformation theory is discussed.

## 1. INTRODUCTION

THE theory of limit analysis employs the model of rigid–perfectly plastic body, and thus cannot account for deformations prior to collapse. For real structures, however, these deformations may sometimes be large enough to influence the equilibrium equations, and to change the load intensity at which the unrestrained plastic flow commences. The influence of changes in geometry can, however, be studied within the framework of the rigid–plastic theory as "the post-yield behavior". One then obtains a sequence of load intensities at which the instantaneous plastic motion of the sequence of deformed structures occurs. The work-hardening being neglected, the load–deflection relations thus are influenced only by the changes in geometry due to plastic deformations. This sort of influence ("secondary effects") has been studied by Onat [1], and certain problems of post-yield behavior of metal rod systems have been solved [2–4]. Existing complete solutions for axially symmetric metal plates are due to Hodge [5] and Lepik [6], and the approximate approach assuming continuation of the initial collapse mode at large deflections has been used in [7, 8].

For reinforced concrete slabs the kinematical approach using the above assumption has been applied by Wood to circular plates [9], whereas Sawczuk [10, 11] and Park [12] treated rectangular plates. For very large deflections, pure membrane analysis has been employed (cf. [13, 14]).

It must be pointed out that the term "secondary effects" (cf. [1]) is misleading when applied to reinforced concrete structures, since in this case small changes in geometry can be of considerable importance. This is due to "the arching action" neglected in both elastic and plastic theories of plates. As first observed by Gvozdev [15], and later discussed by Drucker [16], as well as verified in numerous tests (e.g. [9, 12]), this action can considerably strengthen concrete structures. The arching action is, however, unstable, thus considerations based on the undeformed geometry can lead to erroneous results. For metal plates, the load–deflection curves always keep increasing [6], but for reinforced concrete plates they may decrease appreciably (see Fig. 1).

* At present at: Faculté Polytechnique de Mons, Belgium.

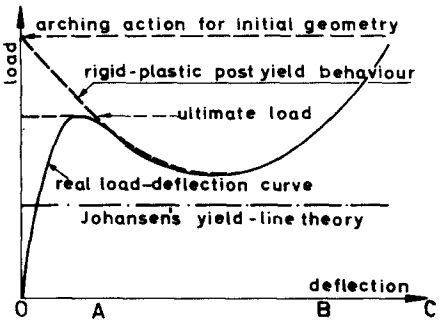


FIG. 1. Load–deflection relations for laterally restrained reinforced concrete slabs.

## 2. KINEMATICAL APPROACH FOR DEFORMED SLABS

The post-yield behavior of reinforced concrete slabs will be analyzed with the following assumptions:

(i) The materials are rigid–perfectly plastic,

(ii) One is interested in approximate solutions based upon the upper-bound theorem of the limit analysis theory,

(iii) The collapse modes adopted do not change with the deformation, i.e. the deflection changes are proportional to one parameter,

(iv) The initial collapse modes are chosen among the yield-line collapse mechanisms.

The upper-bound theorem is valid for structures undergoing negligible changes in geometry prior to the collapse. If it is used in the analysis at large deflections, the routine energy technique has to be applied to the current deformed configuration. Thus, at each stage of the deformation process, the associated kinematic solution can be found and the upper bound for the load–deflection relation can be established. Unfortunately, the real configuration of the deformed system should be known *a priori* at each instant considered. This requirement can rarely be satisfied. Nevertheless, the discussed method is valid in all cases, provided the components of the work equation depend solely upon the deflection at a fixed point. This situation arises, for example, if the yield-line collapse mode assumed is initially exact, and then, due to translation or expansion of plastic hinges, the deformed zones develop into conical surfaces. In a general case, it is not certain that the kinematical approach really gives an upper bound for the load–deflection relation. However, if the considered collapse mode is reasonably close to the real one, errors should not be excessive.

The assumptions stated at the beginning of this section have already been applied in some papers cited in Section 1. However, all the papers dealing with reinforced concrete slabs [9–12] are actually based upon the deformation theory, even if they are written within the framework of the theory of plastic flow.

The difference between the applications of both theories can be easily demonstrated by examining the deformed beam as shown in Fig. 2. For small but finite rotations $\varkappa = w_0 : a$, the position of the undeformed (neutral) layer $O_d$ is determined by $z_d = 0{\cdot}5w_0$ (see [9]). The deformation theory relates stresses to strains, and thus at the point $O_d$ the yield stress

changes sign. However, since the displacements are governed by the rule of rigid-body-motion, the neutral axis for strain rates must coincide with the axis $O_i$ of instantaneous rotation. The principle of vector summation specifies the rotation rate at the hinge, and the axis $O_i$ must therefore lie on the straight line AB, its co-ordinate being $z_i = w_0$. For the flow theory the signs of strain rates and those of stresses must agree, and hence the zone $O_dC$ is in tension. The deformation theory would give there compressive stresses. The rate of energy dissipation is therefore different in the two theories and kinematical approaches based upon them must give different results.

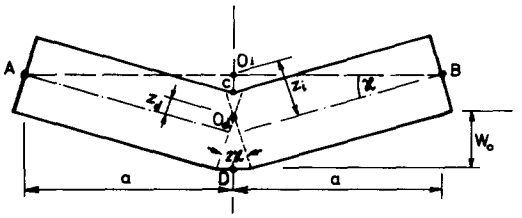


FIG. 2. Yield hinge at large deflections.

Both theories coincide only if deformations vary proportionally in the whole structure. Approximations obtained from the deformation theory can be satisfactory also if the deformation process does not differ strongly from proportionality. Unfortunately, this situation does not occur for slabs, since, as can be seen in Fig. 2, the initially compressed layers become successively stretched during the deformation process. Only for the incipient flow of undeformed structures and at a considerably advanced flow (with both the axes $O_d$ and $O_i$ falling out of the cross-section) will both theories give identical results.

One objection can be raised against adopting the flow theory. The concrete is assumed to be a stable plastic material with the yield point in tension $\sigma_t \to 0$. Thus, the cracked zone is to be considered as undergoing plastic tensile deformations and, whenever the sign of the strain rate changes, the compressive yield stress must appear. However, the compressive strength of the cracked concrete is very small (theoretically equal to zero), until the cracks are closed. Therefore, when cracked zones can possibly turn back to compression the applicability of the flow theory becomes questionable and use of the deformation theory could be considered. However, in the absence of reversed loads, and at collapse modes excluding upward deflections, strain rates decrease monotonically and no change from tensile strains to compressive strains is possible.

## 3. DISSIPATION OF ENERGY IN A PLASTIC HINGE

If a yield-line collapse mode is assumed, no strains but those normal to the cross-section of a plastic hinge can exist, and the only generalized stress resultants are the bending moment $M$ and the axial force $N$. The rate of energy dissipation $\mathrm{d}D$ for an elementary length $\mathrm{d}t$ of a yield line is then:

$$\mathrm{d}D = \dot{\varkappa}(M + z_0 N)\,\mathrm{d}t, \tag{1}$$

where $\dot{\varkappa}$ denotes the curvature rate, and $z_0$ stands for the co-ordinate of the neutral axis of strain rates (the axis of instantaneous reciprocal rotation, Fig. 3(a)). The stress resultants

in the plastic hinge of an arbitrary nonhomogeneous or layered cross-section (Fig. 3b) are:

$$M = \int_{z_0}^{h_l} z\sigma_t(z)\,dz - \int_{-h_u}^{z_0} z\sigma_c(z)\,dz, \qquad N = -\int_{z_0}^{h_l} \sigma_t(z)\,dz + \int_{-h_u}^{z_0} \sigma_c(z)\,dz, \tag{2}$$

where $\sigma_c(z)$, $\sigma_t(z)$ are the yield stresses in compression and tension, respectively.

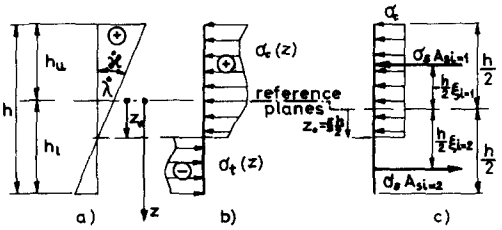


FIG. 3. Strain rate and stress distribution within a plastic hinge; (a) strain rates, (b) yield stresses within an arbitrary non-homogeneous cross-section, (c) reinforced concrete cross-section.

For transversely loaded horizontal slabs, vertical positions of the rotation axes $z_{0j}$ do not influence the work of external loads. Hence, the positions corresponding to the least upper bound to the collapse load must furnish the minimum rate of the total energy dissipation $D$ in the structure, and thus they must be determined from the condition:

$$\frac{\partial D}{\partial z_{0j}} = 0. \tag{3}$$

Since the elementary dissipation $dD$ is non-negative, the absolute minimum of $D$ will be furnished by the values of $z_0$ found from the equation:

$$\frac{\partial(dD)}{\partial z_0} = 0. \tag{4}$$

Introducing equations (1) and (2) into (4), one finds that the latter is equivalent to the assumption of pure bending in plastic hinges ($N = 0$). The least collapse load should then correspond to zero axial forces all over the yield lines. Such a condition is *a priori* satisfied in the yield-line theory (pure bending theory), and Johansen's theory [17] always gives the least upper-bound collapse load possible for the assumed yield-line pattern.

Kinematical restraints, disregarded in the bending theory, rarely permit to satisfy equation (4) all over the slab, even at incipient plastic flow. On the other hand, it is possible to satisfy equation (4) for metal slabs, since the neutral axes for negative and positive pure bending coincide, and the condition $N = 0$ does not contradict kinematical restraints. For reinforced concrete this is impossible, except for the laterally unrestrained slabs; in other cases axial forces (arching action) must be taken into consideration.

For deformed slabs, the position of the neutral axis depends on displacements (Fig. 2) and therefore it may be impossible to have simultaneously $N = 0$ along all plastic hinges. Indeed, upper-bound solutions give in general collapse loads considerably larger than the results from Johansen's theory (see Sections 5 and 6). Only for strips and beams (Section 4)

can the condition (4) be satisfied for a fixed value of the deflection, and then the minimum value of the load–deflection curve (Fig. 1) coincides with the result supplied by the pure bending theory.

To particularize formula (1) for the case of a reinforced concrete cross-section (Fig. 3c), values $\sigma_c(z) = \sigma_c$, $\sigma_t(z) = 0$ for concrete and $\sigma_c(z) = \sigma_t(z) = \sigma_s$, for steel reinforcement have to be introduced into equation (2). Using non-dimensional co-ordinates of the neutral axis $\xi = 2z_0 : h$ and of the $i$th layer of reinforcement (with the area of steel cross-section $A_{si}$) $\xi_i = 2z_i : h$, we can express the elementary rate of energy dissipation as:

$$\mathrm{d}D = |\dot{\varkappa}| M_0 \left( \frac{1+\xi^2}{2} + \xi \operatorname{sgn} \dot{\varkappa} + 2\eta_i |\xi - \xi_i| \right) \mathrm{d}t \quad \text{for } |\xi| \leq 1 \tag{5}$$

$$\mathrm{d}D = |\dot{\varkappa}| M_0 (|\xi| + \xi \operatorname{sgn} \dot{\varkappa} + 2\eta_i |\xi - \xi_i|) \, \mathrm{d}t \quad \text{for } |\xi| \geq 1 \tag{6}$$

where $M_0$ denotes double ultimate bending strength for a unreinforced cross-section, and $\eta_i$ is the reinforcement intensity of the $i$th layer, namely:

$$M_0 = \frac{\sigma_c h^2}{4}, \qquad \eta_i = \frac{\sigma_s A_{si}}{\sigma_c h}. \tag{7}$$

The summation convention applies to repeated subscripts in equations (5) and (6).

## 4. REINFORCED CONCRETE STRIP

The kinematical approach, based on the plastic flow theory (see Section 2), will be applied to the case of a clamped slab strip of span $L$. Reinforcement of arbitrary intensity is assumed to be distributed at the bottom ($\eta_b, \xi_b = 1$) and top face ($\eta_t, \xi_t = -1$) of the slab. At symmetrical loads the motion commences when plastic hinges form at the mid-span and at the supports. If this mode is assumed to continue, the deflection increments are due to rotation rates $\dot{\varphi}$ with respect to the instantaneous axes at supports $O_A$ (Fig. 4).

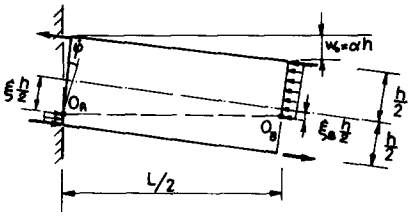


FIG. 4. Stress distribution in plastic hinges at large deflections.

Thus, the rate of work $T$ of uniformly distributed load $q$ and due to the virtual rotation rate $\dot{\varphi}$ is:

$$T = \frac{qL^2}{4}\dot{\varphi} \tag{8}$$

both for the undeformed and deformed states.

Neutral axes in plastic hinges of the deformed strip (Fig. 4) coincide with the axes of reciprocal rotation rates. Hence the relations:

$$\dot{\varkappa}_A = -\dot{\varphi}, \xi_A = \xi; \qquad \dot{\varkappa}_B = 2\dot{\varphi}, \xi_B = \xi - 2\alpha \tag{9}$$

define the strain rates due to the virtual rotation rate $\dot{\varphi}$.

Introducing the adopted reinforcement characteristics, together with relations (9), into (5) for both support and midspan hinges, we obtain the total rate of dissipation for a unitary width of the strip:

$$D = 2D_A + D_B = M_0\dot{\varphi}[(1-\xi)^2 + (1+\xi-2\alpha)^2 + 8(\eta_t+\eta_b) + 8(\eta_t-\eta_b)(\alpha-\xi)]. \tag{10}$$

Since the external work does not depend on the position of rotation axis, the balance equation $T = D$ furnishes the least bound to collapse load, when the dissipation rate attains a minimum, that is when:

$$\frac{\partial D}{\partial \xi} = 0. \tag{11}$$

Condition (11) furnishes

$$\xi = \alpha + 2(\eta_b - \eta_t) \tag{12}$$

and the work equation yields the collapse load:

$$\frac{qL^2}{8M_0} = 4(\eta_b+\eta_t) - 4(\eta_b-\eta_t)^2 + (1-\alpha)^2 \tag{13}$$

The result (13) holds for $\xi \leq 1$ and $\xi_B \geq -1$, i.e. for

$$\alpha \leq \alpha_1 = 1 - 2|\eta_b - \eta_t|. \tag{14}$$

When this value is exceeded, formula (6) must be used instead of (5) for the support or the midspan hinge, depending on the sign of the expression $(\eta_b - \eta_t)$. The minimum condition (11) is satisfied for $\xi = 1$ or $\xi_B = -1$, respectively, and the collapse load is:

$$\frac{qL^2}{8M_0} = 4(\eta_b+\eta_t) + 2(1-\alpha)^2 - 4(1-\alpha)(\eta_b-\eta_t). \tag{15}$$

For a more advanced deformation ($\alpha > \alpha_2 = 1$) the formula (6) must be applied to all hinges, and $\xi$ turns out not to influence the work equation. The collapse load is then expressed by the linear relation:

$$\frac{qL^2}{8M_0} = 4\alpha(\eta_b+\eta_t). \tag{16}$$

The collapse load is plotted versus central deflection in Fig. 5, for various configurations of reinforcement. The minimum value of the collapse load:

$$\frac{q_Y L^2}{8M_0} = 4(\eta_b+\eta_t) - 2(\eta_b-\eta_t)^2, \tag{17}$$

is obtained for $\alpha = \alpha_0 = 1 - |\eta_b - \eta_t|$. It is equal to the collapse load supplied by the yield-line theory, since (according to Section 3) the state $\alpha = \alpha_0$ corresponds to pure bending ($N = 0$) in all hinges.

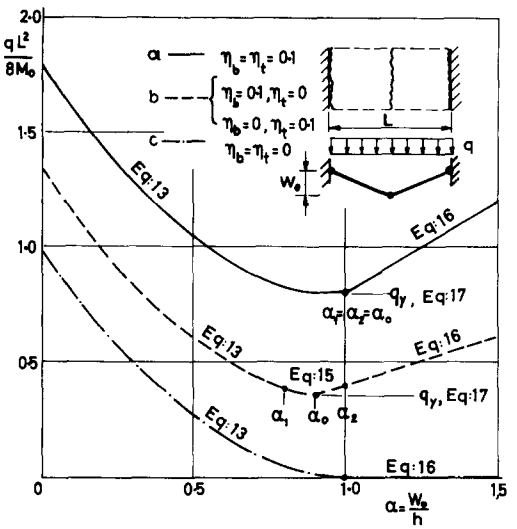


FIG. 5. Load–deflection curves for clamped reinforced concrete strips: (a) symmetrically reinforced, (b) singly reinforced, (c) unreinforced.

It is known that the energy method is equivalent to so called "equilibrium method" in the kinematical approach. In the equilibrium method the work equation corresponds to the moment equilibrium, and the minimum condition (11) represents the equilibrium of horizontal forces acting in the hinges. This method seems to be more illustrative, since different collapse-load expressions can be associated with different plastic regimes met by stress profiles at the interaction curve. For the cross-section considered (and $\eta_b > \eta_t$) the interaction curve is shown in Fig. 6. For relatively small rotations $\varphi = 2w_0 : L$, the axial forces can be assumed constant throughout the strip. Thus, the stress profile remains vertical and it moves from the initial position $A_1B_1$ up to the state of maximum tensile action. Since the structure considered is symmetric, the initial vertical locations of neutral axes must be the same in the support and in the midspan hinges. Thus for both hinges the plastic flow vectors $\vec{\varepsilon}(\dot{\varkappa}, \dot{\lambda} = z_0\dot{\varkappa})$ must be parallel. This requirement, together with the normality condition, specifies the initial position of the stress profile $A_1B_1$.

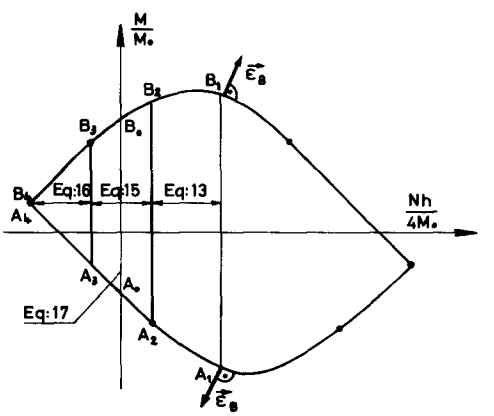


FIG. 6. Interaction curve for doubly reinforced concrete cross-section.

All the load–deflection relations presented are valid also for loads other than uniformly distributed, provided they produce the maximum moment at the midspan of the undeformed strip. Only the left sides of the formulae must be replaced by expressions corresponding to the rate of work of the actually considered external load. There is, however, one difference. For a concentrated load applied at the midspan, the solution presented is exact, i.e. the yield criterion is not violated in the rigid regions. For distributed loads this condition is satisfied as long as the axial force remains compressive. For larger deflections the plastic hinge moves out of the cross-section (see [4], for steel plates) and the employed collapse mode furnishes only an upper bound to the limit load.

## 5. CIRCULAR CLAMPED SLAB

Consider a circular slab of radius $R$ uniformly and doubly isotropically reinforced (thus $\eta_b = \eta_t = \eta$). The reinforcements are placed at the top ($\xi_t = -1$) and at the bottom ($\xi_b = 1$) faces. The initial conical collapse mode, of Fig. 8, is assumed to apply even as the deflections increase.

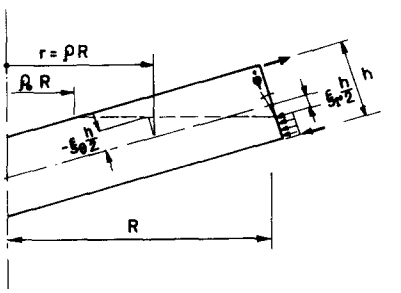


FIG. 7. Radial section of deformed circular slab.

If the formulae (5), (6) for the dissipation rate are to be applied, a continuous strain field must be considered as a yield-line pattern. The adjacent radial yield lines make then the angle $d\theta$. Thus, a virtual rotation rate about the axis $O$ at the clamped edge (Fig. 7) produces in the support hinge the following deformations:

$$\dot{\varkappa}_r = -\dot{\varphi}, \qquad \xi_r = \xi. \tag{18}$$

For the conically deformed surface one obtains

$$\dot{\varkappa}_\theta = \dot{\varphi}\, d\theta, \qquad \xi_\theta = \xi - 2\alpha(1-\rho), \tag{19}$$

where $\rho = r:R$ denotes a dimensionless radial co-ordinate, and $\alpha = w_0:h$ stands for a dimensionless central deflection. For a virtual rotation rate $\dot{\varphi}$, the elementary work of the uniformly distributed load $q$ is:

$$T = \frac{qR^3}{6}\dot{\varphi}\, d\theta. \tag{20}$$

Since the deformations vary along the radial hinges, the total dissipation rate for an elementary segment $d\theta$ takes eventually the form:

$$D = M_0\dot{\varphi}\left\{\frac{(1-\xi_r)^2}{2}+4\eta+\int_0^1\left[\frac{(1+\xi_\theta)^2}{2}+4\eta\right]d\rho\right\}R\,d\theta. \tag{21}$$

After integrations, the minimum condition (11) applied to the expression (21) gives $\xi = 0{\cdot}5\alpha$. The virtual work equation $T = D$ yields the collapse load:

$$\frac{qR^2}{6M_0} = 1+8\eta-\alpha+\frac{5}{12}\alpha^2. \tag{22}$$

The formula (22) is valid for $\xi_r \leq 1$, $\xi_\theta \geq -1$, i.e. for $\alpha \leq \alpha_1 = 2{:}3$. For larger deflections a membrane zone spreads from the centre and the formulae (6) and (5) must be applied for $0 < \rho \leq \rho_0$ and $\rho_0 \leq \rho < 1$, respectively. The boundary radius $\rho_0$ is specified by the condition $\xi_\theta = -1$, which gives:

$$\rho_0 = -\frac{1+\xi}{2\alpha}. \tag{23}$$

Integrating the dissipation and employing the appropriate formulae for each zone, one obtains

$$\frac{qR^2}{6M_0} = 2\left(1-\frac{1+\xi}{2}\right)^2+4\eta\left[2+\frac{3}{\alpha}\left(\frac{1+\xi}{2}-\alpha\right)^2\right]+\frac{(1+\xi)^3}{12\alpha}, \tag{24}$$

whereas the minimum criterion (11) gives:

$$\frac{1+\xi}{2} = \sqrt{[(6\eta+\alpha)^2+2\alpha(6\eta+1)]}-(6\eta+\alpha). \tag{25}$$

Expression (25) is valid for $\xi < 1$, i.e. for

$$\alpha \leq \alpha_2 = 1+\frac{1}{12\eta}, \tag{26}$$

but there is no need to establish new formulae for larger deflections. The minimum principle (11) is identical to the condition of equilibrium for horizontal forces. Considering a slab segment with central angle $\theta = \pi$, we can see that, if $\xi > 1$, the radial forces in the support hinge cannot be balanced by the resultant of circumferential stresses acting along the diameter. Thus, once the rotation axis attains the bottom face, it must remain there for $\alpha > \alpha_2$. Thus formula (24) is still valid. Introducing $\xi = 1$ instead of the value given by (25), we obtain:

$$\frac{qR^2}{6M_0} = 4\eta\left[2+\frac{3}{\alpha}\left(1-\alpha\right)^2\right]+\frac{2}{3\alpha}. \tag{27}$$

In Fig. 8, the collapse loads for reinforcement intensity $\eta = 0{\cdot}1$ are plotted vs. the central deflection. It can be seen, that the minimum load is considerably larger than

$$\frac{q_Y R^2}{6M_0} = 8\eta, \tag{28}$$

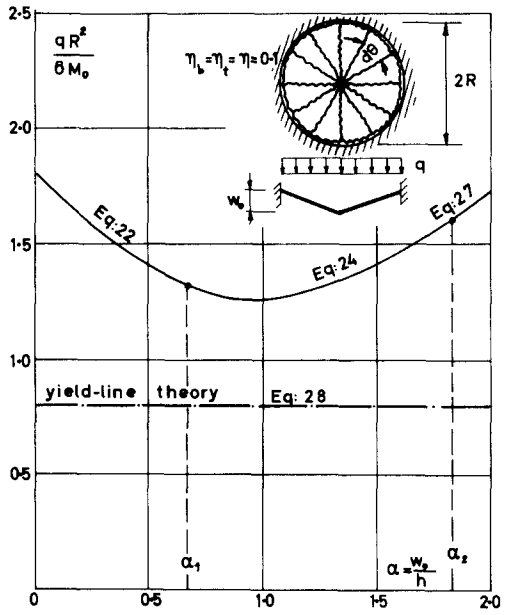


FIG. 8. Load–deflection curve for symmetrically reinforced circular clamped slab.

as given by the yield-line theory. It is clear that the coincidence observed for the slab strip cannot occur here.

## 6. SQUARE SLAB

Considerations concerning a circular plate can be directly applied to the case of a square clamped slab. Assuming the diagonal collapse mode (Fig. 9) to be preserved at large deflections, the rate of external work of the uniformly distributed load $q$ is found to be

$$T = \frac{qL^2}{6}\dot{\varphi}. \tag{29}$$

As in the case of the deformed circular slab, strains vary along the diagonal hinges (see Fig. 7), and the deformation rates are:

$$\dot{\varkappa}_S = -\dot{\varphi}, \qquad \xi_S = \xi, \qquad \dot{\varkappa}_D = \sqrt{2}\dot{\varphi}, \qquad \xi_D = \xi - 2\alpha\left(1 - \frac{t\sqrt{2}}{L}\right). \tag{30}$$

Subscripts $S$ and $D$ correspond to the support and to the diagonal yield lines, respectively, and $t$ is the coordinate measured from the slab centre along the diagonal hinge.

The slab is assumed to be reinforced only at its bottom face. Then, introducing the reinforcement characteristics and the relations (30) into the dissipation formula (5), and performing the integration, we obtain the total dissipation rate $D$. It reaches minimum

for $\xi = 2\eta + 0{\cdot}5\alpha$. The work equation $T = D$ now yields the collapse load:

$$\frac{qL^2}{48M_0} = \frac{1-\alpha}{2} + \frac{5}{24}\alpha^2 + 2\eta(1-\eta). \tag{31}$$

The obtained formula is valid for $\xi_S \leq 1$ and $\xi_D \geq -1$, and it gives the following limitations for the central deflection:

$$\alpha \leq \alpha_1 = 2(1-2\eta), \qquad \alpha \leq \alpha_2 = \tfrac{2}{3}(1+2\eta). \tag{32}$$

Whenever $\alpha_1 < \alpha < \alpha_2$, the formula (6) ought to be applied when evaluating the dissipation in the boundary hinges. One can see, however, that the equilibrium of horizontal thrusts acting on a triangular panel cannot be satisfied if $\xi > 1$. Thus, $\xi = 1$ must be introduced in the original formula from which the expression (31) was derived, and eventually we obtain

$$\frac{qL^2}{48M_0} = 1 - \alpha(1-\eta) + \frac{\alpha^2}{3}. \tag{33}$$

For the central deflection $\alpha > \alpha_3 = 1$, the formula (6) must be applied in the inner zone of diagonal hinges whenever

$$t < \frac{L}{\sqrt{2}}\left(1 - \frac{1}{\alpha}\right). \tag{34}$$

Since the condition $\xi = 1$ must still hold, we obtain:

$$\frac{qL^2}{48M_0} = \alpha\eta + \frac{1}{3\alpha}. \tag{35}$$

When the second of conditions (32) is more restrictive, $(\alpha_1 > \alpha > \alpha_2)$, a membrane zone appears for

$$t < \frac{L}{\sqrt{2}}\left(1 + \frac{1+\xi}{2\alpha}\right) \tag{36}$$

when $\xi < 1$. Then, applying the formula (5) to the support hinges and to the outer part of diagonals, and the formula (6) to the inner part, we obtain a total dissipation rate which attains a minimum for

$$\xi = \alpha^{\frac{1}{2}}[\alpha + 2(1+2\eta)]^{\frac{1}{2}} - \alpha - 1. \tag{37}$$

When the minimum of $D$ is introduced into the work equation, the load–deflection relation becomes

$$\frac{qL^2}{48M_0} = (1+\alpha)^2 - \frac{\alpha^2}{3} - \frac{2}{3}\alpha^{\frac{1}{2}}[\alpha + 2(1+2\eta)]^{\frac{3}{2}} + \eta(4+5\alpha). \tag{38}$$

When the deflection exceeds the value

$$\alpha_4 = \frac{1}{4\eta}, \tag{39}$$

the neutral axis remains at the bottom face ($\xi = 1$), and thus, the expression (35) is again valid.

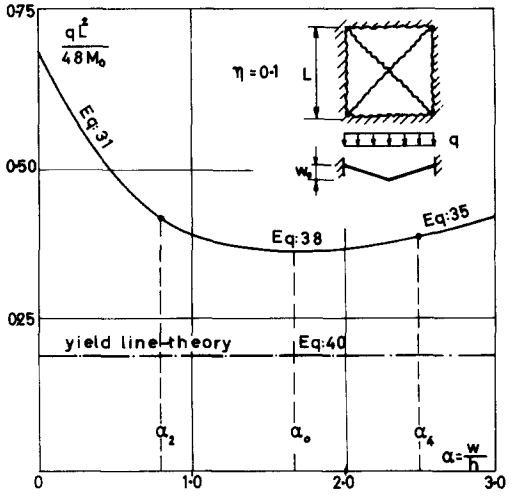


FIG. 9. Load–deflection curve for square clamped symmetrically reinforced slab.

For reinforcement intensity $\eta = 0{\cdot}1$, the collapse load is plotted in Fig. 9 vs. the central deflection. Similarly to the case of a circular slab, the minimum load, though being considerably smaller than the initial load, is larger than that provided by the yield-line theory:

$$\frac{q_Y L^2}{48 M_0} = \eta(2-\eta). \tag{40}$$

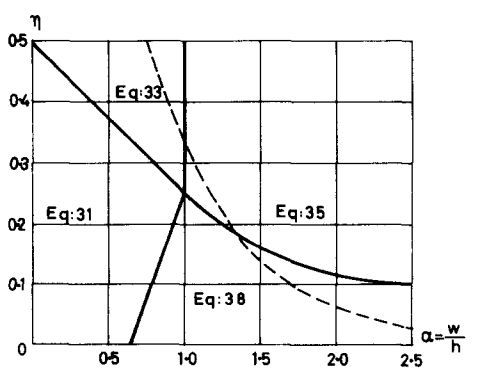


FIG. 10. Square clamped slab; ranges of validity of solutions.

Regions of applicability of expressions (31–38) are shown in Fig. 10, where the dashed line indicates the deflection values for which the minimum load is attained.

## 7. FINAL REMARKS

The load–deflection curve for rigid plastic structures being decreasing (zone OA in Fig. 1), for the reasons of safety the geometry changes prior to the initial plastic flow should be taken into consideration. If they are not accounted for, the classical pure bending theory [17] should be preferentially applied. For clamped or laterally restrained reinforced concrete slabs, this theory occurs to be kinematically non-admissible (see [18]) but it gives a safe approximation of the collapse load. On the other hand, the rigid–plastic analysis, kinematically correct but based upon the initial geometry, can lead to a considerable overestimation of the real carrying capacity.

If the ultimate collapse load (the peak value) is desired, the analysis must account for the elastic–plastic response. If it does not, it must be accompanied by experiments specifying approximate values of deflections associated with the peak load [14]; otherwise the minimum ordinate should stand for the ultimate collapse load.

Variations of a yield mechanism due to the changes in geometry, disregarded in the paper, are of importance for metal plates. For reinforced concrete structures, however, the yield mechanism is of a more stable character. In fact, the collapse mode maintains its original form up to rather large deflections. This situation is due to the fact that membrane forces are always tensile in metal slabs, whereas reinforced concrete structures are compressed in the early stage of deformation. For example, the positive plastic hinge must move out of the midspan cross-section of a uniformly loaded clamped metal strip, whereas for a reinforced concrete structure the maximum moment conserves its initial position until the membrane force becomes tensile.

*Acknowledgements*—The author wishes to thank Professor Marcel Save (Faculté Polytechnique de Mons) and Professor Antoni Sawczuk (Université de Grenoble and Polish Academy of Sciences) for their valuable discussions, critical remarks, and help throughout the preparation of this paper.

## REFERENCES

[1] E. T. ONAT, The influence of geometry changes on the load–deformation behavior of plastic solids, Plasticity. *Proc. 2nd Symp. Naval Structural Mech.* p. 225, Pergamon Press (1960).
[2] E. T. ONAT and L. S. SHU, Finite deformations of a rigid perfectly plastic arch. *J. appl. Mech.* **29**, 549 (1962).
[3] M. JANAS, Plastic analysis of rib gridwork at large deflections (in Polish). *Archwm Inżyn. ladow.* **11**, 95 (1965).
[4] R. M. HAYTHORNTHWAITE, Mode change during the plastic collapse of beams and plates. *Development in Mechanics*, Vol. 1. Plenum Press (1961).
[5] P. G. HODGE, *Limit Analysis of Rotationally Symmetric Plates and Shells*. Prentice-Hall (1963).
[6] Ü. R. LEPIK, Plastic flow of thin rigid–plastic circular plates (in Russian). *Izv. Akad. Nauk USSR Mekh. i Mash'stroen* 78, No. 2 (1960).
[7] E. T. ONAT and R. M. HAYTHORNTHWAITE, The load-carrying capacity of circular plates at large deflection. *J. appl. Mech.* **23**, 49 (1956).
[8] A. R. RZHANITSYN, The design of plates and shells by the kinematical method of limit equilibrium. IX$^{e}$ *Congr. Int. de Méc. Appliqueé* **6**, 331, Université de Bruxelles, Bruxelles (1957).
[9] R. H. WOOD, *Plastic and Elastic Design of Slabs and Plates*. Thames & Hudson (1961).
[10] A. SAWCZUK and L. WINNICKI, Plastic behavior of simply supported concrete plates at moderately large deflections. *Int. J. Solids Struct.* **1**, 97 (1965).
[11] A. SAWCZUK, Membrane action in flexure of rectangular plates with restrained edges. *Flexural Mechanics of Reinforced Concrete, Proc. Int. Symp. Miami*, p. 347, Am. Soc. civ. Engrs (1965).
[12] R. PARK, Ultimate strength of rectangular concrete slabs under short-term uniform loading with edges restrained against lateral movement. *Proc. Inst. civ. Engrs* **28**, 125 (1964).
[13] L. G. JAEGER, An approximate analysis for plating panels under uniformly distributed load. *Proc. Inst. civ. Engrs* **10**, 137 (1958).

[14] R. PARK, Tensile membrane behavior of uniformly loaded rectangular reinforced concrete slabs with fully restrained edges. *Mag. Concr. Res.* **16**, 39 (1964).
[15] A. A. GVOZDEV, The basis for paragraph 33 of the Reinforced Concrete Design Code, (in Russian). *Stroit. Prom.* **17**, 51 (1939).
[16] D. C. DRUCKER, On structural concrete and the theorems of limit analysis. *Publs. int. Ass. Bridge struct. Engng* **21**, 49 (1961).
[17] K. W. JOHANSEN, *Yield-Line Theory*. Cement and Concrete Ass. (1962).
[18] M. JANAS, Kinematical compatibility problems in the yield-line theory. *Mag. Concr. Res.* **19**, 33 (1967).

(*Received* 27 *December* 1966; *revised* 29 *May* 1967)

**Абстракт**—В работе приводится пластический анализ железобетонных пластинок с учетом влияния мембранных усилии и изменении геометрии конструкции, возникающих при больших прогибах. Исползуя теорию течения жёстко-, пластических тел, получены соотношения между прогибом и нагрузкой в целом процессе деформации: начиная от осевого сжатия возникающего при наличии горизонтальных опорных связей (эффект распора), до мембранного растяжения и трещинообразования. Исползуется кинематический подход с применением энергетического метода или метода равновесия; схема разрушения считается неизменимой в процессе нагружения. Приводится примеры для балочной защемленной плиты, для круглых и квадратных пластинок и сравнивается предложенный метод с анализом исползующим деформационную теорию пластичности.